Deliyannis, Theodore L. et al "Simulation of LC Ladder Filters Using Opamps"
Continuous-Time Active Filter Design
Boca Raton: CRC Press LLC,1999

Chapter 6

Simulation of LC Ladder Filters Using Opamps

6.1 Introduction

In Chapter 5, we examined two general methods of high-order filter design, namely the cascade of low-order sections and the multiple-loop feedback method. We will now explain ways for the simulation of passive LC ladder filters as an alternative but, at the same time, popular and very useful approach to active RC filter design.

For reasons that we will explain in Section 6.2, the passive LC filter in the form of a ladder has to be resistively terminated as shown in Fig. 1.19, repeated here as Fig. 6.1 for convenience. The transfer voltage ratio of this filter obtained from Table 1.2 is as follows:

$$H(s) = \frac{V_o}{V_2} = \frac{Z_{21}R_L}{(R_s + Z_{11})(R_L + Z_{22}) - Z_{21}Z_{22}} \tag{6.1}$$

where Z_{ij}, $i, j = 1, 2$ are the z-parameters of the LC two-port.

Clearly, a filter function can be realized by this circuit, provided that it is written in the form of Eq. (6.1), so that the LC two-port parameters can be suitably identified and subsequently synthesized. The terminating resistances are taken into consideration during the design, and their ratio influences the amount of signal power transferred from source to load via the LC two-port.

In this chapter, we do not intend to design the LC two-port, as this has been done long ago for all the filter functions that have been obtained as the solution to the approximation problem. The values of the inductors and capacitors for various orders and R_L/R_s ratios of these functions have been tabulated and appear in many text and reference books [1–4].

The purpose of this chapter is to explain some ways for simulating either the impedance of the inductors or the operation of the passive LC ladder by means of active RC circuits. Thus, in Section 6.2, we give the motivation for using the simulation of the LC ladder filter in order to obtain useful high-order active RC filters. In Sections 6.3 and 6.4, we use gyra-

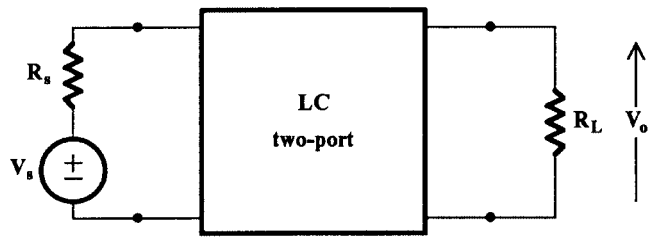

FIGURE 6.1
Resistively terminated LC two-port.

tors and generalized-immittance converters, first introduced in Chapter 3, to simulate the impedance of the inductors and the supercapacitors, the latter appearing in the passive ladder through a suitable impedance transformation of the prototype filter. Next, in Section 6.5, the method of simulating the actual operation of the passive ladder filter is presented.

6.2 Resistively-Terminated Lossless LC Ladder Filters

We are interested here in LC filters that are in the form of an LC ladder resistively terminated at both ends, as is shown in Fig. 6.2. In this circuit, X_i, $i = 1, 2, \ldots, n$ are LC impedances or admittances. X_1 and/or X_n may be missing, in some cases.

The important characteristic of the ladder is that there is a single path of signal transmission from source to load. Orchard has shown [5] that when the ladder is properly designed, at the frequencies of maximum power transfer, the first-order sensitivity of the magnitude of the transfer function to each inductor and capacitor is zero, while it remains low in the intermediate frequencies throughout the passband. This can be intuitively explained as follows: since the LC ladder is lossless at the frequencies of maximum power transfer, a change in an L or a C value can only increase the loss of the filter. Thus, the derivative of the frequency response (magnitude) with respect to each L and each C will be zero at these frequencies and so will be the corresponding sensitivity.

Furthermore, it has been shown [6, 7] that, for this type of filter, the sensitivity to the inductors and capacitors can be near zero throughout the passband rather than at only a few frequencies. It is therefore logical to expect that this low sensitivity of the lossless ladder filter will be retained in an active RC network which simulates the "operation" of the LC ladder or which contains active RC subcircuits that simulate the impedance of the inductances. This idea has resulted in the popularity of this method in active RC filter design.

It should be mentioned that the sensitivity of the ladder LC filter is not low in the transition and stopbands. However by proper design [6, 7] this can be close to a lower bound. On the other hand, as long as the loss in these bands remains higher than the filter requirements dictate, this sensitivity will not be of any practical importance.

6.3 Methods of LC Ladder Simulation

The simulation of a resistively terminated LC ladder can be achieved by the following four methods:

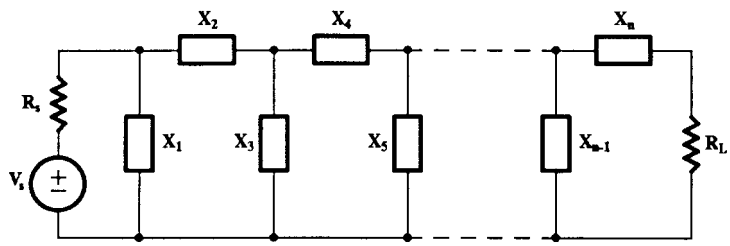

FIGURE 6.2
A resistively terminated ladder network.

1. Inductance substitution by a gyrator-C combination.
2. Impedance transformation of part or the whole of the LC ladder. In this case generalized-immitance converters are employed.
3. Simulation of currents and voltages in the ladder. The leapfrog (LF), coupled-biquad (CB) as well as the signal-flow-graph methods are names that have been used in the past to express essentially the same method.
4. The linear transformation (LT), which includes the wave active filter (WAF) method, approaches the simulation of the LC ladder the same way as *c*, but it uses transformed variables instead of simulating the voltages and currents of the LC ladder.

Methods 1 and 2 are usually considered to constitute the topological approach to LC ladder simulation, whereas the last two (3 and 4) constitute the functional or operational approach. In this chapter, we will explain the first three of these methods, while the fourth will be treated in the next chapter.

6.4 The Gyrator

The gyrator was introduced in Section 3.3. It is, in effect, a positive impedance inverter defined by its transmission matrix as follows:

$$[A] = \begin{bmatrix} 0 & \pm 1/g_2 \\ \pm g_1 & 0 \end{bmatrix}$$

Its symbol is shown again in Fig. 6.3(a). If it is terminated at port 2 in an impedance Z, Fig. 6.3(b), the impedance seen at port 1 will be

$$Z_1 = \frac{1}{g_1 g_2} \cdot \frac{1}{Z} \tag{6.2}$$

Clearly g_1, g_2 have the dimensions of a conductance and are called, most appropriately, gyration conductances. For inductance simulation, Z will be the impedance of a capacitor C, when Z_1 becomes, from (6.2)

$$Z_1 = s\frac{C}{g_1 g_2} = s\, L_{eq} \tag{6.3}$$

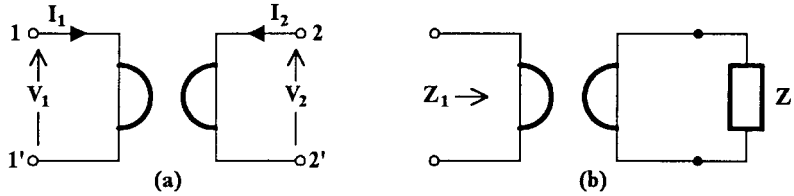

FIGURE 6.3
(a) The gyrator symbol and (b) the gyrator terminated in an impedance Z at port 2.

where

$$L_{eq} = \frac{C}{g_1 g_2} \tag{6.4}$$

The gyrator, strictly speaking, is an active two-port. However, if

$$g_1 = g_2 = g$$

it behaves as a lossless passive one, since then the power flowing in, $V_1 I_1$, is equal to the power flowing out, $V_2(-I_2)$, from the gyrator. However, the active gyrator, depending on the value of g_1/g_2, will act as an amplifier for the signal in one direction and as an attenuator in the opposite direction.

In the ideal case, we consider g_1 and g_2 independent of frequency which, in practice, is true only for a limited frequency range.

It can be seen from Fig. 6.3(b) that this simulated inductance seen at port 1 is grounded. However, in lowpass, bandpass, and bandstop LC ladders, floating inductors, i.e., inductors not connected to ground, are present. To simulate such an inductor, two gyrators are required to be connected as shown in Fig. 6.4. The two gyrators have to be matched; otherwise, this arrangement will not simulate a pure floating inductance.

The quality of the simulated inductor depends greatly on the quality of the capacitor C. Thus, if g_c is the leakage conductance of the capacitor, then the associated loss resistance RL of the simulated inductor can be calculated from Eq. (6.2) as follows:

$$Z_1 = \frac{1}{g_1 g_2} \cdot \frac{1}{Z_c} = \frac{1}{g_1 g_2}(sC + g_c)$$

Thus,

$$L_{eq} = \frac{C}{g_1 g_2}, \qquad R_L = \frac{g_c}{g_1 g_2} \tag{6.5}$$

Clearly, g_c should be as small as possible.

6.4.1 Gyrator Imperfections

Let us assume that the gyrator in Fig. 6.5 is not ideal and that its admittance matrix is as follows:

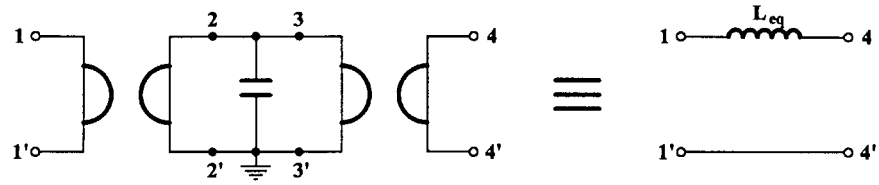

FIGURE 6.4
Use of two gyrators to simulate a floating inductor.

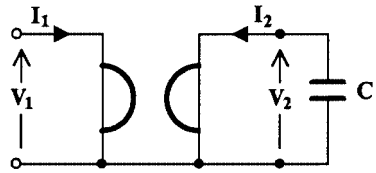

FIGURE 6.5
Nonideal gyrator terminated in a capacitor.

$$[Y] = \begin{bmatrix} g_a & g_1 \\ -g_2 & g_b \end{bmatrix} \tag{6.6}$$

where g_a, g_b are non-zero, pure conductances. Since

$$I_2 = -sCV_2$$

straightforward analysis gives that the input impedance Z_{in} will be the following:

$$Z_{in} \equiv \frac{V_1}{I_1} = \frac{sC + g_b}{g_a(sC + g_b) + g_1 g_2} \tag{6.7}$$

Substituting $j\omega$ for s, we get

$$Z_{in}(j\omega) = \frac{j\omega C g_1 g_2 + g_b(g_1 g_2 + g_a g_b) + \omega^2 C^2 g_a}{(g_1 g_2 + g_a g_b)^2 + \omega^2 C^2 g_a^2} \tag{6.8}$$

Thus, the input impedance represents the series connection of an inductance L_{eq} and an unwanted resistance R_u, where

$$L_{eq} = \frac{C g_1 g_2}{(g_1 g_2 + g_a g_b)^2 + \omega^2 C^2 g_a^2} \tag{6.9}$$

$$R_u = \frac{g_b(g_1 g_2 + g_a g_b) + \omega^2 C^2 g_a}{(g_1 g_2 + g_a g_b)^2 + \omega^2 C^2 g_a^2} \tag{6.10}$$

Therefore, the quality factor Q of the simulated inductance is finite, while both L_{eq} and its associated resistance R_u are functions of ω^2. Using Eqs. (6.9) and (6.10) this quality factor can be determined to be

$$Q = \frac{L_{eq}\omega}{R_u} = \frac{C g_1 g_2 \omega}{g_b(g_1 g_2 + g_a g_b) + \omega^2 C^2 g_a} \tag{6.11}$$

which has the following maximum value Q_{max}:

$$Q_{max} = \frac{g_1 g_2}{g_1 g_2 + g_a g_b}\sqrt{1 + \frac{g_1 g_2}{g_a g_b}} \tag{6.12}$$

The value of Q_{max} is independent of frequency and the capacitance C (provided the capacitor is ideal) and occurs at the following frequency:

$$\omega_o = \frac{1}{C}\sqrt{(g_1 g_2 + g_a g_b)\frac{g_b}{g_a}} \tag{6.13}$$

Thus, for high-quality simulated inductances, the gyrator parasitic conductances g_a, g_b should be as small as possible compared to g_1, g_2.

6.4.2 Use of Gyrators in Filter Synthesis

It is implied from the above discussion that the gyrator-capacitor combination can take the place of an inductor in the LC ladder. As an example, consider the third-order highpass filter shown in Fig. 6.6(a). Let $g_1 = g_2 = 10^{-3}S$.

The capacitance required for the simulation of the 30 mH inductance will be determined using Eq. 6.4. Thus, solving for C, we get

$$C = g_1 g_2 L_{eq} = 10^{-6} \times 3 \times 10^{-2} F = 30 \text{ nF}$$

The circuit using the simulated inductance is shown in Fig. 6.6(b).

LC ladders most suitable for inductance simulation using gyrators are those with no floating inductors in their structure. Such are highpass filters and bandpass filters with no transmission zeros in the upper stopband. The structures of these types of filters are shown in Fig. 6.7(a) and (b), respectively.

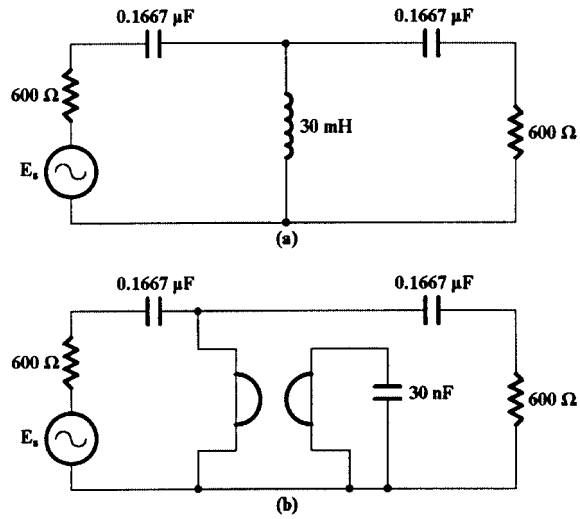

FIGURE 6.6
(a) Simulation of the inductance in an LC filter using (b) a gyrator-capacitor combination.

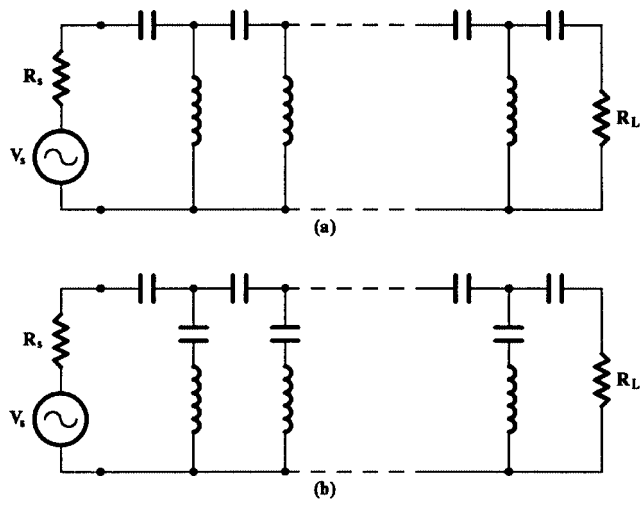

FIGURE 6.7
Optimum ladder structures for inductance simulation using gyrators: (a) highpass and (b) bandpass with no transmission zeros in the upper stopband.

It should be mentioned that the impedance-inverting property of the gyrator can be used to transform an RC impedance to an RL impedance. For example, consider the gyrator terminated at port 2 by the RC impedance

$$Z_{RC} = R = \frac{1}{sC} \tag{6.14}$$

The impedance presented at its input will be

$$Z_{in} = \frac{1}{g_1 g_2} \cdot \frac{1}{Z_{RC}}$$

or

$$Z_{in} = \frac{1}{g_1 g_2} \cdot \frac{1}{R + \dfrac{1}{sC}} = \frac{1}{g_1 g_2} \cdot \frac{sC}{sCR + 1} \tag{6.15}$$

Clearly, Z_{in} represents the equivalent impedance of a resistance $(1/Rg_1g_2)$ in parallel with an inductance (C/g_1g_2), as the reader can easily see.

This suggests that a filter function can be decomposed into an RC impedance (or admittance) function and an RL impedance (or admittance) function, the latter being realized as the input impedance (or admittance) at one port of a gyrator terminated by the appropriate RC impedance (or admittance) at the other port. Then, the two impedances (or admittances) are combined to give the overall circuit using a gyrator, resistors and capacitors. This method of using the gyrator in the synthesis of active RC networks was very popular in the 1960s, when saving in active elements was considered a figure of merit in active RC filter design. This is not so true today, though, when the low price of the opamps allows for the relaxation of this condition in favor of resorting to simpler methods of active RC synthesis such as the inductance simulation method.

6.5 Generalized Impedance Converter, GIC

The concept of the GIC was introduced in Section 3.3. As a reminder, it is a two-port defined by its transmission matrix

$$[A] = \begin{bmatrix} k & 0 \\ 0 & k/f(s) \end{bmatrix} \tag{6.16}$$

where $f(s)$ is the impedance conversion function and k a positive constant.

The GIC is very useful in LC ladder filter simulation by active RC networks, when it is used either as a positive-impedance converter (PIC) or to produce a frequency-dependent negative resistance of type-D (D-FDNR). In the first case, $f(s) = s$, and the GIC is terminated at port 2 by a resistance R. Then, the input impedance at port 1 is the following:

$$Z_{i1} = f(s)Z_L = sR \tag{6.17}$$

This is recognized as the impedance of an inductance R, in henries.

On the other hand, if $f(s) = 1/s$ and a capacitor C is connected across port 2, the input impedance at port 1 will be

$$Z_{i1} = \frac{1}{s} \cdot \frac{1}{sC} = \frac{1}{s^2C} \tag{6.18}$$

This is recognized as an FDNR of type-D, which is a negative resistance in effect, since, if $j\omega$ is substituted for s in Eq. (6.18), Z_{i1} becomes

$$Z_{i1} = -\frac{1}{\omega^2 C} \tag{6.19}$$

which is resistive, negative, and frequency dependent.

It is usual to give the GIC the symbol shown in Fig. 6.8 with the dot always indicating the side of port 1 and the conversion function $f(s)$ written inside the box.

6.5.1 Use of GICs in Filter Synthesis

According to the previous discussion, a GIC with conversion function $f(s) = s$ and a resistor connected across its port 2 presents in its port 1 the impedance of an inductor (Fig. 6.9), thus operating as a PIC.

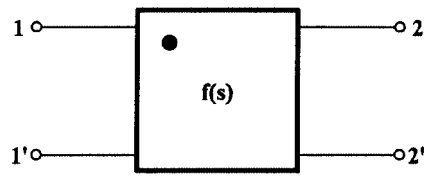

FIGURE 6.8
Usual symbol of the GIC.

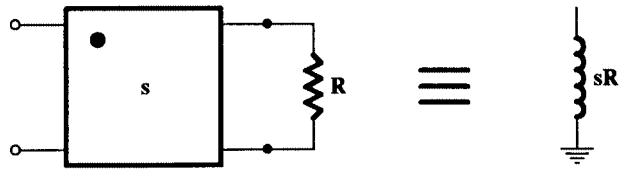

FIGURE 6.9
The GIC operating as PIC.

Two matched GICs of this type are required in order to simulate a floating inductance as shown in Fig. 6.10. This is in agreement with the corresponding case for gyrators.

Following this approach, we can say that optimum ladders for inductance simulation are, as in the case of gyrators, highpass filters, and bandpass filters with no zeros of transmission in the upper stopband. These filter structures are shown in Fig. 6.7(a) and (b), respectively. This type of inductance simulation technique was first introduced by Gorski-Popiel [8].

It has been shown [9] that the optimum GIC circuit for this application is that shown in Fig. 6.11 terminated at port 2 by the resistance R_5. The conversion function of this GIC can be easily shown (Section 3.5.2) to be the following:

$$\frac{V_1}{I_1} = sCRR_5 = ks \tag{6.20}$$

with

$$k = CRR_5 \tag{6.21}$$

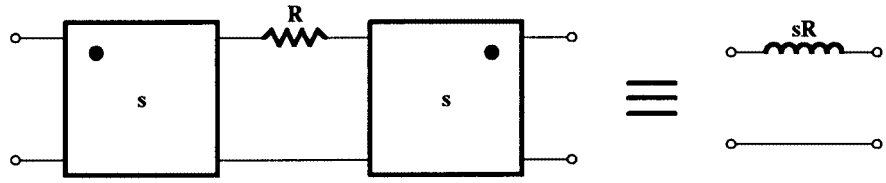

FIGURE 6.10
Simulation of a floating inductor.

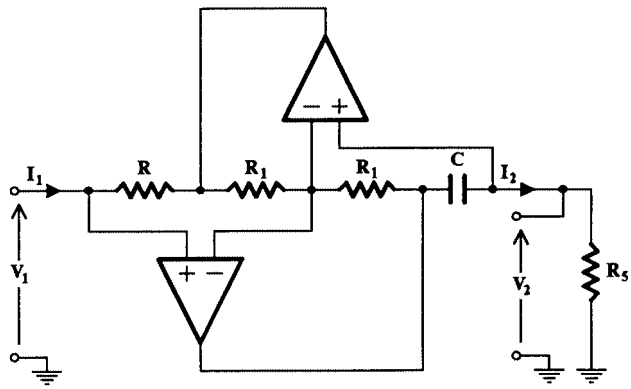

FIGURE 6.11
Most practical GIC circuit for inductance simulation used as a PIC.

Extending this, it can be shown [8, 10], that any $(n + 1)$-terminal network consisting of inductors can be simulated only using n GICs and a resistive network of the same topology. The importance of this statement is that it can lead to savings in the numbers of GICs required in the simulation of LC ladder filters, provided that such subnetworks can be separated from the corresponding ladders.

Consider, for example, the ladder filter in Fig. 6.12(a). The inductor subnetwork is as shown in Fig. 6.12(b) and can be simulated using three GICs [Fig. 6.12(c)] instead of five that would have been required otherwise (two for each floating inductor and one for L_3, the position of which can be exchanged with that of C to avoid its being floating).

As a second example, consider realizing a bandpass active filter from the Butterworth third-order lowpass filter

$$F(s) = \frac{1}{s^3 + 2s^2 + 2s + 1}$$

From tables [1, 2] or otherwise, we get the passive realization in LC ladder form shown in Fig. 6.13(a). Since there is a floating inductance in the circuit, two gyrators or two GICs are required for its realization arranged as is shown in Fig. 6.4 and Fig. 6.10, respectively.

From this, we can obtain the bandpass filter by applying the usual lowpass-to-bandpass transformation to the reactive components (Section 2.6.3)

$$s_n \Rightarrow \frac{\omega_o}{B}\left(\frac{s^2 + \omega_o^2}{\omega_o s}\right)$$

For $\omega_o = 1$ krad/s, $B = 100$ rad/s and an impedance level of 600 Ω, the sixth-order bandpass LC ladder filter will be as shown in Fig. 6.13(b). Clearly, it is preferable, for reasons of economy, to simulate this filter using PICs as is depicted in Fig. 6.13(c), since using gyrators

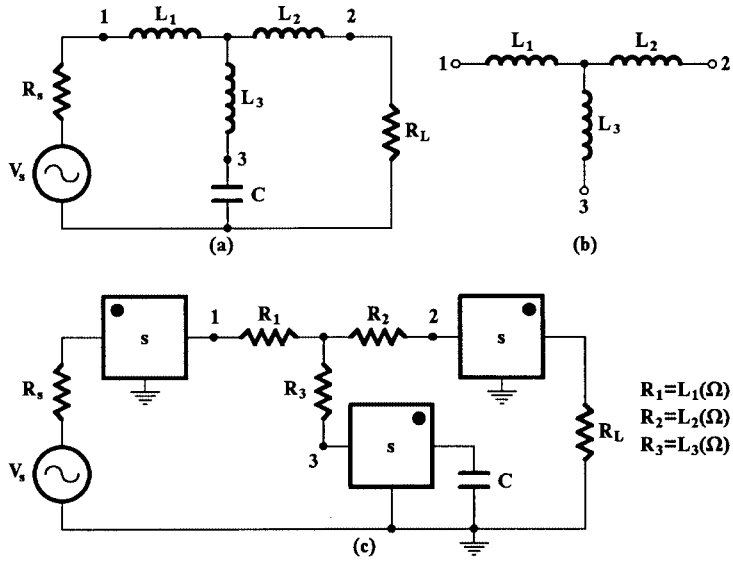

FIGURE 6.12
The LC ladder in (a), with the LC subnetwork in (b) simulated in (c) using GICs as PICs.

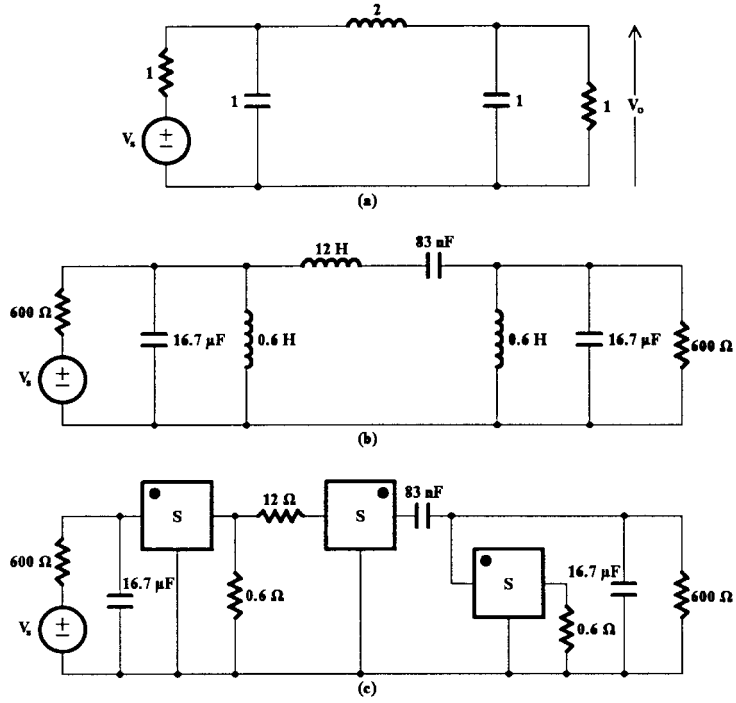

FIGURE 6.13
The third-order Butterworth lowpass filter in (a) is transformed into the bandpass in (b), which is simulated using PICS as in (c).

would require a larger number of opamps to be employed for the simulation. Notice that this simulated circuit employs three resistances of very low values, which make the circuit impractical. If the values of the terminating resistances can be raised further without any effect on the use of the circuit, the impedance level of the whole filter can be raised to make all the component values practical. On the other hand, if the terminating resistance values have to remain 600 Ω, the conversion constant k of the PICs will be smaller than 1, i.e., 10^{-3}, which will lead to increased resistance values of the PICs terminated resistors, namely 600 Ω and 12 kΩ instead of 0.6 Ω and 12 Ω, respectively.

One should note here that the PICs used in the simulation of the inductance subnetwork must be matched. Two different inductance subnetworks may employ for their simulation two different sets of PICs, but all the PICs in each set should be matched.

It can be seen that, by changing the inductance-subnetwork to the topologically similar resistive subnetwork using PICs, we have in effect performed a complex impedance scaling on part of the LC ladder. Complex impedance scaling of the whole ladder is explained immediately below.

6.6 FDNRs: Complex Impedance Scaling

This technique of inductance simulation has been treated extensively by Bruton [11]. It is most suitable for lowpass filters of the minimum capacitor realization. The reason for this will become apparent below.

Bruton's technique amounts to complex impedance scaling of the entire filter and not to part of it as we saw in the case of using PICs. It is based on the fact that the filter transfer function will remain unchanged if the impedance of each element is divided by the same quantity, in this case by s. We can demonstrate this simulation approach by means of an example.

The filter in Fig. 6.12(a) is scaled by dividing each impedance by s. Then, the resistance is transformed to the impedance of a capacitance, while the impedance of the capacitor is transformed to the impedance of a *supercapacitor* (Section 3.3.1), as is shown in Fig. 6.14(a). The simulated circuit is shown in Fig. 6.14(b), where a FDNR D-element is used to simulate the supercapacitor.

A GIC circuit useful in realizing the FDNR D-element is shown in Fig. 6.15, terminated in a capacitor C_5. It can be easily shown that its input admittance is

$$\frac{I_1}{V_1} = s^2 C_1 C_5 R_4 \tag{6.22}$$

In cases where the capacitive terminations of the ladder are undesirable in Fig. 6.14(a), we can use two extra PICs terminated by two resistances R_s and R_L, as shown in Fig. 6.16.

Comparing the circuit in Fig. 6.14(b) to that in Fig. 6.12(c), it can be seen that the former requires fewer opamps than the latter, but its terminations are capacitive. However, if this is unacceptable, because of the existence of a source impedance or a resistive load, buffer

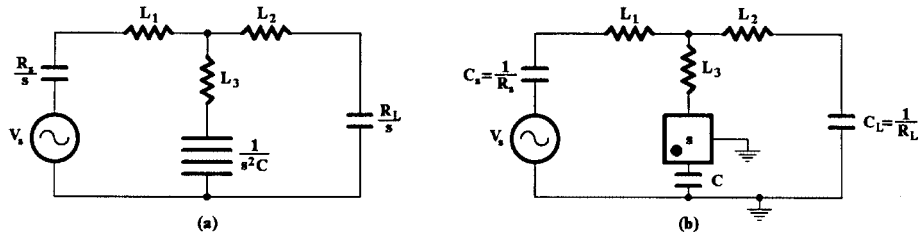

FIGURE 6.14
(a) Transformation of the ladder in Fig. 6.12(a) to another employing a D-element, which is realized by a GIC with $f(s) = s$ terminated in a capacitor (b).

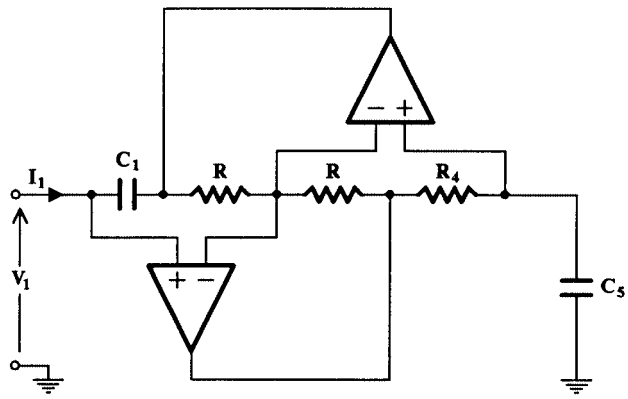

FIGURE 6.15
A useful FDNR D-element.

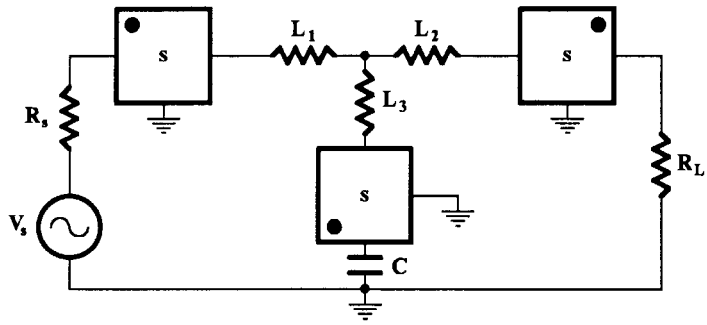

FIGURE 6.16
Realization of the ladder of Fig. 6.12(a) using a D-element and resistive terminations.

amplifiers can be used in the circuit, one between the signal source and the $1/R_s$ capacitor and the other between capacitor $1/R_L$ and the load resistance. This approach avoids using the circuit in Fig. 6.16, which employs three GICs also.

Lowpass LC ladder filters can be designed using either a minimum number of inductors or a minimum number of capacitors [1]. Of the two, the latter, when simulated using Bruton's transformation, leads to a filter with minimum number of D-elements, thus saving opamps. Unfortunately, this is not true in the case of bandpass filters, where there is no saving in opamps, even as compared to the PIC design.

One serious practical problem with this ladder simulation technique is that there is no dc return path for the noninverting inputs of the two opamps in the FDNR circuit embedded in the circuit in Fig. 6.14(b). To avoid this, one solution [9] is to connect two large resistors, as large as practically possible, in parallel with the two terminating capacitors C_s and C_L. Their values should be chosen such that the required value of the transfer function at dc will not change. To demonstrate this, let R_a and R_b be the two resistances connected across the capacitors C_s and C_L, respectively, in Fig. 6.14(b). The value of V_o/V_s at dc is equal to 0.5 for all equally terminated lowpass LC ladders of interest. Therefore, the voltage drop across R_b should be $V_s/2$, which means that at dc

$$\frac{V_o}{V_s} = \frac{R_b}{R_a + L_1 + L_2 + R_b} = 0.5 \tag{6.23}$$

from which we get

$$R_b = R_a + L_1 + L_2 \tag{6.24}$$

6.7 Functional Simulation

In this approach to ladder simulation [12, 13], we seek to simulate the "operation" of the LC ladder, i.e., the equations that describe the topology of the LC ladder, rather than simulate the impedance of the inductances. In other words, instead of using an active circuit that simulates the impedance sL of inductance L, we try to simulate the voltage and the current that exist in sL, which are related by

$$I = \frac{V}{sL} \tag{6.25}$$

In so doing, we use voltages that are analogous to each inductor current and voltage. For example, we can simulate the above I, V relationship, by means of an integrator with time constant dependent on L, the output voltage of which is analogous to I.

Similarly, we treat the operation of a capacitance C. Here, an integrator with time constant dependent on C will be used to integrate a voltage, which is analogous to current I, in order to produce another voltage V according to the relationship

$$V = \frac{I}{sC} \tag{6.26}$$

It will be recalled that we use integrators, and not differentiators, for reasons related to the excessive noise behavior of the latter.

The functional simulation method that we are to explain here is known as the leapfrog (LF) method, because it leads to a circuit structure resembling that of the so-named children's game (see Fig. 5.5).

We will explain the LF method by means of an example. Consider the fifth-order lowpass filter shown in Fig. 6.17(a), where all node voltages as well as the currents in the inductors have been suitably named. We write the relationships connecting these currents and the node voltages using Kirchhoff's current rule as well as Ohm's law. Referring to node No. 1, we have

$$\frac{V_s - V_1}{R_s} - sC_1V_1 - I_2 = 0$$

which can be also written as follows:

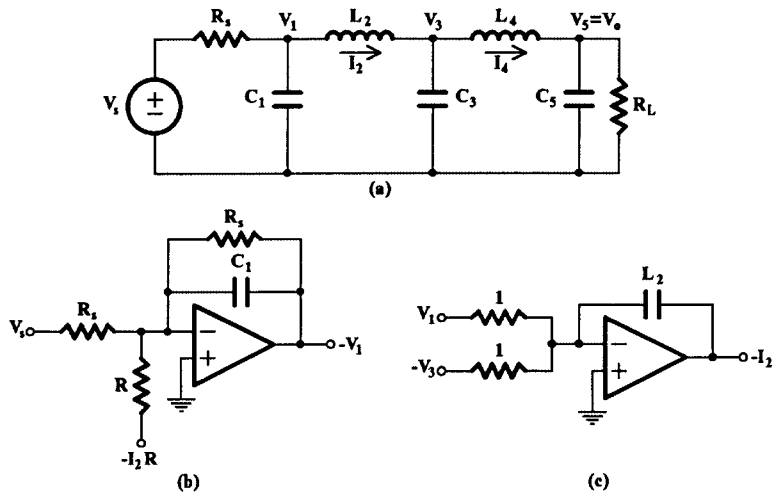

FIGURE 6.17
Fifth-order lowpass filter.

$$-V_1 = \frac{1}{sC_1}\left(\frac{V_s - V_1}{R_s} - I_2\right) \tag{6.27}$$

Thus, $-V_1$ can be obtained at the output of an inverting lossy integrator as shown in Fig. 6.17(b). In a similar way, we may write for I_2

$$-I_2 = -\frac{1}{sL_2}(V_1 - V_3) \tag{6.28}$$

Then, a voltage analogous to $-I_2$ can be obtained at the output of a lossless inverting integrator, in which the capacitance in farads is arithmetically equal to the value of L_2 in henrys. This is shown in Fig. 6.17(c).

Working on an analogous basis, we will obtain the rest of the required equations, which are as follows:

$$V_3 = -\frac{1}{sC_3}(I_4 - I_2) \tag{6.29}$$

$$I_4 = -\frac{1}{sL_4}(V_5 - V_3) \tag{6.30}$$

$$-V_5 = -\frac{1}{sC_5}\left(I_4 - \frac{V_5}{R_L}\right) \tag{6.31}$$

Clearly, V_3 and I_4 will be obtained at the output of lossless integrators, while $V_5(=V_o)$ at the output of a lossy integrator.

In building up the overall active RC ladder, it is usually helpful to produce it first in block diagram form and then insert the integrators and the other components in the places of the corresponding blocks. Thus, from Eqs. (6.27) through (6.31), we obtain the block diagram shown in Fig. 6.18.

It can be seen that integrators, sign changers, and summers are required for the implementation. However, summation of voltages can either be performed by the integrators or by the sign changers, preferably the former. Following this, we can now proceed to produce the actual active RC ladder. This is shown in Fig. 6.19.

It can be seen that the "horizontal" branches of the active ladder consist of inverting integrators alternating with inverting integrators and sign inverters in cascade, the latter being in effect noninverting integrators. The top and bottom integrators are lossy, because of the passive ladder terminating resistors, while the rest are lossless integrators.

In the case of a ladder of even order, the last capacitor will be missing [C_5 in Fig. 6.17(a)]. Then, the current in the last L will also pass through the load resistor R_L, which will give rise to a simple V, I relationship. Thus, in the case of Fig. 6.17(a) with C_5 missing the load end of the ladder would be as shown in Fig. 6.20(a). We will then have

$$-I_4 = \frac{1}{R_L}(-V_5) \tag{6.32}$$

and the active RC ladder would terminate as it is shown in Fig. 6.20(b).

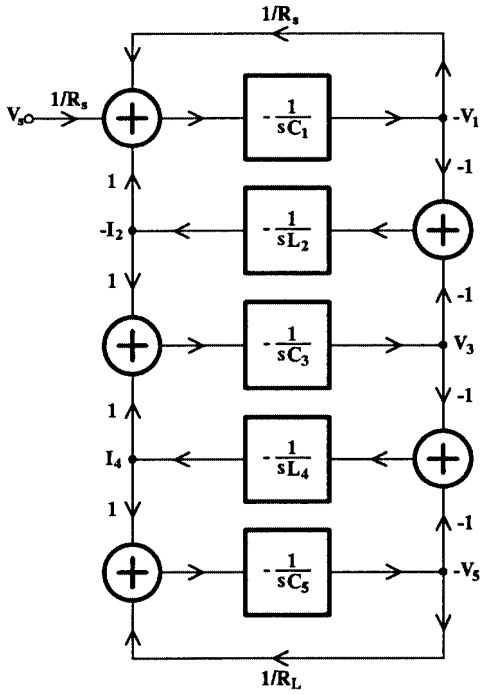

FIGURE 6.18
Block diagram of the active ladder simulating the operation of the filter in Fig. 6.17(a).

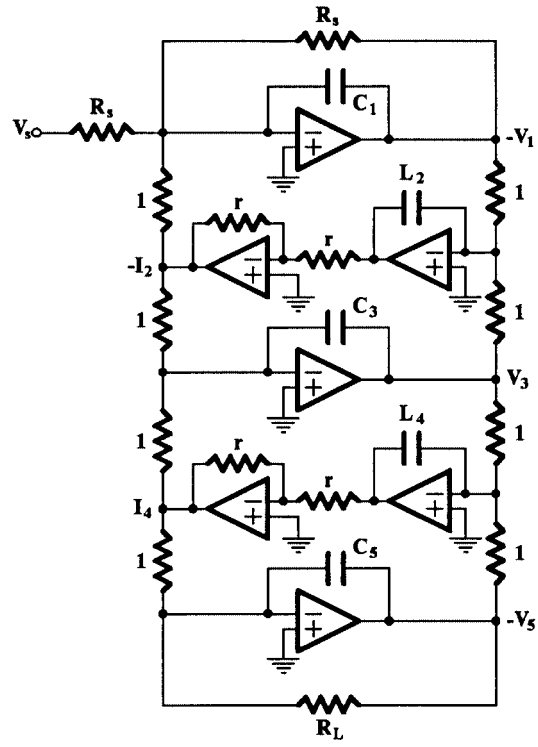

FIGURE 6.19
The overall LF or active RC ladder simulating the operation of the LC ladder filter in Fig. 6.17(a).

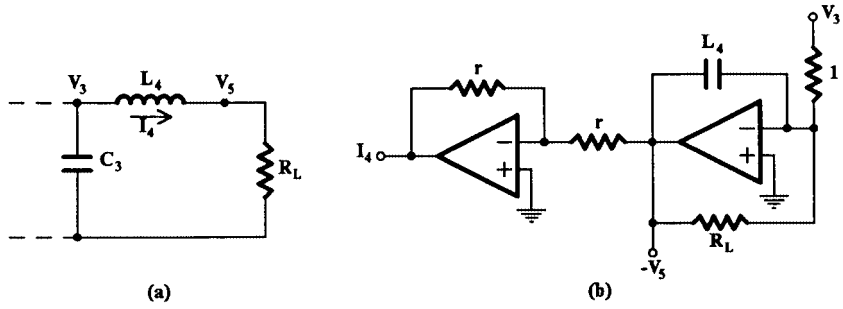

FIGURE 6.20
When capacitor C_5 in Fig. 6.17(a) is missing (a), the last branch of the active ladder will be as in (b).

6.7.1 Example

As an example, let us consider the realization of the third-order Butterworth lowpass function in the form of an LF structure. The lowpass prototype LC filter terminated by equal resistances in a normalized form is as shown in Fig. 6.21. Following the procedure outlined above, we find first the equations for voltages V_1, V_2 and current I_2. These are as follows:

$$-V_1 = -\frac{1}{sC_1}\left(\frac{V_s - V_1}{R_s} - I_2\right)$$

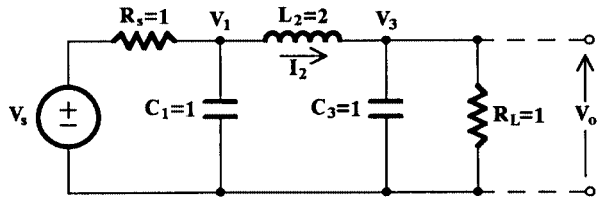

FIGURE 6.21
The lowpass LC filter of third-order.

$$-I_2 = -\frac{1}{sL_2}(V_1 - V_3)$$

$$V_3 = -\frac{1}{sC_3}\left(\frac{V_3}{R_L} - I_2\right)$$

Then, the LF structure in block diagram form, as well as the practical circuit, will be as shown in Fig. 6.22(a) and (b), respectively. The circuit in Fig. 6.22(b) can be denormalized to any convenient impedance level and any required cutoff frequency.

The use of so many inverting and noninverting integrators in the active ladder inevitably creates problems due to the excess phase associated with each of them. These are more pronounced at higher frequencies and require attention. We can use the methods explained in Section 4.9 and compensate the integrators, particularly the noninverting ones, since the excess phase created by them is higher than that created by the inverting integrators.

6.7.2 Bandpass Filters

Applying the usual lowpass-to-bandpass transformation

$$s_n = \frac{s^2 + \omega_o^2}{sB}$$

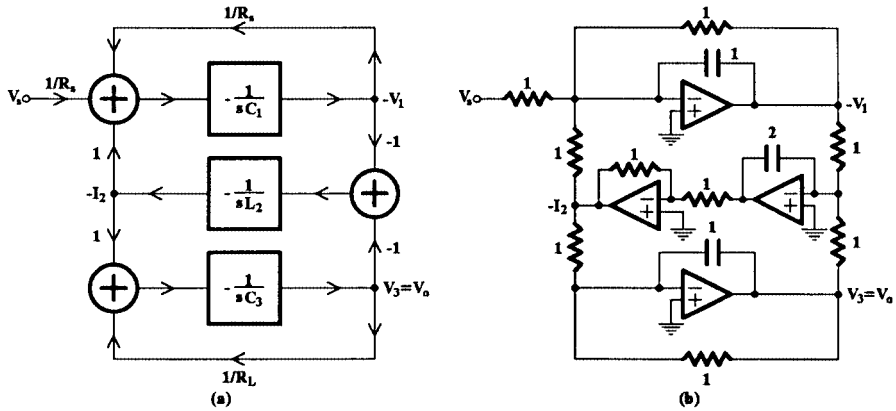

FIGURE 6.22
LF simulation of the third-order Butterworth lowpass LC filter shown in Fig. 6.21.

to the block diagram in Fig. 6.18, each integrator block will be transformed to a biquad of infinite Q factor, apart from the two lossy integrators at the beginning and the end of the ladder, which will have finite Q factors. We can redraw the block diagram of the general form shown in Fig. 5.5 repeated here in Fig. 6.23.

The bandpass filters obtained this way are geometrically symmetric or all-pole, as they are often called. Szentirmai [14] has generalized the method so that it can realize almost any filter function, i.e., bandpass and band-reject filters, which are not symmetrical, having arbitrary stopband requirements. If the bandpass filter is symmetrical, then all biquads can be chosen to resonate at the same frequency, which gives the circuit the characteristic of modularity.

The LF in its general form with each $t_i(s)$ block being a biquad is usually called the coupled-biquad structure (CB). The infinite-Q biquadratics will be in practice realized by biquads that can be adjusted to have as high a Q factor as possible. In many cases, we can use SABs, but in some cases, three-opamp biquads (see Chapter 4) may be more suitable. However, in the latter case, the number of opamps becomes excessive while, if these are not compensated for their excess phase, there will be serious distortion in their frequency response, when they operate at higher frequencies (say, above 100 kHz).

The LF active filters retain the low-sensitivity characteristic of the passive ladder in the passband, while in the transition or stopbands they are no better than the corresponding cascade filter.

As an example of obtaining a geometrically symmetric bandpass filter from a lowpass active ladder, let us apply the transformation

$$s_n \Rightarrow 10\left(\frac{s^2+1}{s}\right)$$

to the integrators of the lowpass filter in Fig. 6.22(a).

The two lossy integrators have the same transfer function

$$t_1(s), t_3(s) = -\frac{1}{s+1} \tag{6.33}$$

while the lossless one in the middle, being noninverting, has the transfer function

$$t_2(s) = \frac{1}{2s} \tag{6.34}$$

Applying the above lowpass-to-bandpass transformation to Eqs. (6.33) and (6.34) gives the following biquadratic functions, respectively:

$$T_1(s), T_3(s) = -\frac{0.1s}{s^2+0.1s+1} \tag{6.35}$$

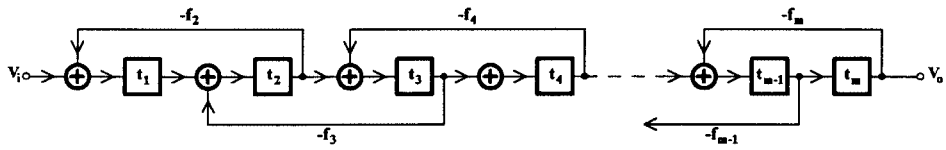

FIGURE 6.23
The leapfrog structure, repeated.

$$T_2(s) = \frac{1}{20}\,\frac{s}{s^2+1} \tag{6.36}$$

Each one of T_1 and T_3 may be realized by the sign-inverting bandpass SAB in Fig. 4.10 or by the three-opamp Åkerberg-Mossberg biquad. However for the realization of T_2 a non-inverting bandpass biquad is required that is capable of having an infinite Q factor. Such a biquad can be either the Åkerberg-Mossberg suitably modified [9] or the Sallen and Key [15] bandpass biquad. Also, the SAB in Fig. 4.10 could be used followed by or, better, following a sign inverter.

If we choose to use the SAB in Fig. 4.10, T_1 and T_3, being identical, will be realized by the SAB in Fig. 6.24(a) and T2 by the circuit in Fig. 6.24(b). These biquads are then coupled according to the scheme in Fig. 6.25 to obtain the overall bandpass filter. Each biquad in this figure can be denormalized to the required center frequency ω_o and to a suitable impedance level. Note that the gain of the filter is 0.5 as in the LC prototype.

6.7.3 Dynamic Range of LF Filters

We have pointed out in Chapter 5 that the dynamic range of high-order active filters is an important characteristic of the various structures and should always be maximized during

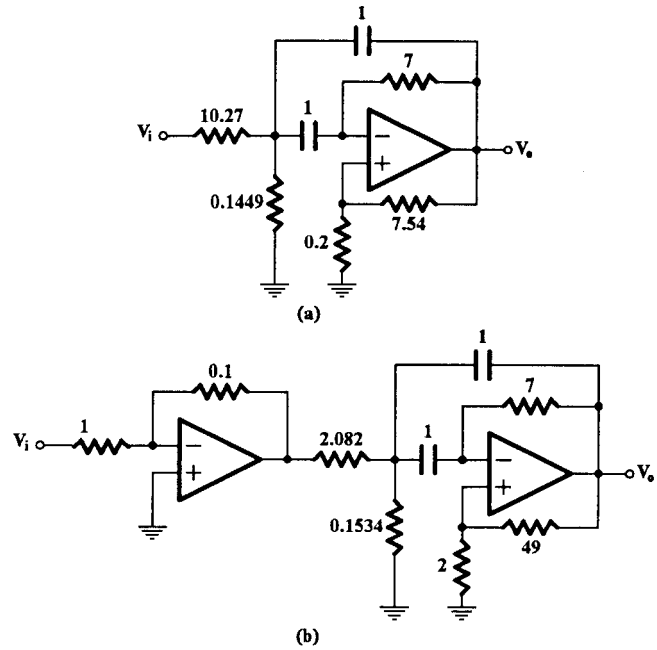

FIGURE 6.24
Realization of (a) T_1 and T_3, Eq. (6.33) and (b) of T_2, Eq. (6.34).

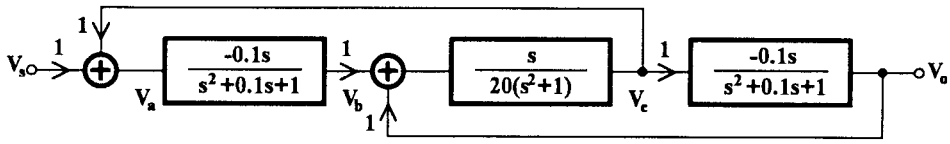

FIGURE 6.25
The overall LF or CB filter realizing the sixth-order Butterworth bandpass function.

the design stage. Luckily, the LF ladder can be adjusted for maximum dynamic range. For this purpose, one tries to adjust the gain of each t_i block to obtain the same maximum value at the output of every opamp in the circuit. Then the value of each feedback ratio f_i is changed to the value that keeps the product $f_i t_{i-1} t_i$ unchanged.

This is an advantage of the LF over the GIC-type simulation, where optimization of the dynamic range can be achieved only by properly intervening during the phase of the original passive synthesis [9].

6.8 Summary

The simulation of a resistively terminated ladder LC filter is desirable, because it leads to active RC filters with very low sensitivity in the passband. This simulation can be achieved either by simulating the inductances by means of opamps, resistors and capacitors, or by simulating the operation of the ladder. The opamps in the first case are used to realize gyrators, GICs (PICs), or FDNRs. In the second case, the opamps are used as integrators, lossless and lossy, summers, and sign-reversing elements (LF) or as parts of active biquads (CB).

The low passband sensitivity of the filters designed using the latter simulation approach is their most important characteristic. This allows for looser tolerances of the components when trimming these filters.

Another very important advantage of this kind of active RC filters is the availability of the prototype ladder LC designs. The well known lowpass Butterworth, Chebyshev, Bessel, and Cauer filter functions have been designed as resistively terminated ladder LC filters and tabulated. From these tables, using the element transformation table of Section 2.7.1 other filter types (namely highpass, bandpass, and bandstop) can be obtained, depending on the requirements. Of course, this does not prevent anyone from designing a custom ladder LC filter, something that one must certainly do when the requirements call for the design of an equalizer.

The main important disadvantages of the ladder simulation method are the following:

1. The large number of opamps required which, apart from the economical problem associated with it, leads to high dc power consumption, thus creating heat in the circuit. In some cases though, the number of opamps required may be reduced if the use of one-opamp grounded gyrators and FDNRs [16, 17] can satisfy the filter requirements.
2. The limited dynamic range of the filters obtained by the topological method of simulation. This is not important in the case of the LF type of simulation since, as we have mentioned, maximization of the dynamic range of the corresponding circuits is possible. In the case of the topological method of simulation, maximizing the dynamic range is rather involved and should be applied during the design of the passive ladder circuit.

References

[1] L. Weinberg. 1962. *Networks Analysis and Synthesis,* New York: McGraw-Hill.
[2] A. I. Sverev. 1967. *Handbook of Filter Synthesis,* New York: John Wiley and Sons.

[3] E. Christian and E. Eisenman. 1966. *Filter Design Tables and Graphs,* New York: John Wiley & Sons.
[4] J. K. Skwirzynski. 1965. *Design Theory and Data for Electrical Filters,* Princeton, NJ: D. Van Nostrand.
[5] H. J. Orchard. 1966. "Inductorless filters," *Electron. Lett.* **2**, pp. 224–225.
[6] M. L. Blostein. 1963. "Some bounds on sensitivity in RLC networks," *Proc. 1st Allerton Conf. on Circuits and System Theory,* Urbana, Illinois, pp. 488–501.
[7] G. C. Temes and H. J. Orchard. 1973. "First order sensitivity and worst-case analysis of doubly terminated reactance two-ports," *IEEE Trans. on Circuit Theory* **20**(5), pp. 567–571.
[8] J. Gorski-Popiel. 1967. "RC-active synthesis using positive-immittance converters," *Electron. Lett.* **3**, pp. 381–382.
[9] A. S. Sedra and P. O. Brackett. 1979. *Filter Theory and Design: Active and Passive,* London: Pitman.
[10] A. Antoniou. 1970. "Novel RC-active network synthesis using generalized-immittance converters," I*EEE Trans. on Circuit Theory* CT-17, pp. 212–217.
[11] L. T. Bruton. 1980. *RC-Active Circuits: Theory and Design,* Englewood Cliffs, NJ: Prentice-Hall.
[12] F. E. I. Girling and E. F. Good. 1970. "Active filters 12. The leap-frog or active ladder synthesis," *Wireless World* **76**, pp. 341–345.
[13] F. E. I. Girling and E. F. Good. 1970. "Active filters 13. Applications of the active ladder synthesis," *Wireless World* **76**, pp. 445–450.
[14] G. Szentirmai. 1973. "Synthesis of multiple-feedback active filters," *Bell Syst. Tech. J.* **52**, pp. 527–555.
[15] R. P. Sallen and E. L. Key. 1955. "A practical method of designing RC active filters," *IRE Trans. Circuit Theory* CT-2, pp. 74–85.
[16] H. J. Orchard and A. N. Wilson, Jr. 1974. "New active gyrator circuit," *Electron. Lett.* **10**, pp. 261–262.
[17] C. E. Schmidt and M. S. Lee. 1975. "Multipurpose simulation network with a single amplifier," *Electron. Lett.* **11**, pp. 9–10.